Supporting Information

Conformationally Confined Three-Armed Supramolecular Folding for Boosting Near-Infrared Biological Imaging

Hui-Juan Wang,[ab] Meng-Meng Zheng,[a] Wen-Wen Xing,[a] Yongxue Li,[a] Yao-yao Wang,[b] Hongjie Zhu,[b] Ying-Ming Zhang,*[a] Qilin Yu,*[c] Yu Liu*[ade]

a College of Chemistry, State Key Laboratory of Elemento-Organic Chemistry, Nankai University, Tianjin 300071, P. R. China; b Shandong Provincial Key Laboratory of Chemical Energy Storage and Novel Cell Technology, School of Chemistry and Chemical Engineering, Liaocheng University, Liaocheng 252000, P. R. China; c Key Laboratory of Molecular Microbiology and Technology, College of Life Sciences, Nankai University, Tianjin 300071, P. R. China; d Haihe Laboratory of Sustainable Chemical Transformations, Tianjin 300192, P. R. China; e Collaborative Innovation Center of Chemical Science and Engineering, Tianjin 300192, P. R. China.

E-mail: ymzhang@nankai.edu.cn; yuqilin@nankai.edu.cn; yuliu@nankai.edu.cn

Table of Contents

1. Material and methods

All the reagents and solvents were commercially available and used as received without further purification. Column chromatography was performed on silica gel (200-300 mesh). NMR spectra were recorded on Bruker AV400 instrument at 298 K and chemical shifts were recorded in parts per million (ppm). High-resolution mass spectra (HR-MS) were measured on a Q-TOF LC-MS and MALDI-TOF-HRMS. UV/vis spectra were recorded on a Shimadzu UV-3600 spectrophotometer equipped with a PTC-348WI temperature controller. Photoluminescence and lifetimes were recorded by FS5 instrument (Edinburg Instruments, Livingstone, UK). Photoluminescence spectra at different temperature were recorded by FLS1000 equipped with Optistat DN. The samples for transmission electron microscope (TEM) measurements were prepared by dropping the solution onto copper grids and then air-dried. The samples were examined by a high-resolution TEM (Tecnai G2 F20 microscope, FEI) equipped with a CCD camera (Orius 832, Gatan) operating at an accelerating voltage with a CCD camera (Orius 832, Gatan) operating at an accelerating voltage of 200 kV. Scanning electron microscopy (SEM) was performed on ZEISS Merlin Campact scanning electron microscope and JSM-7500F scanning electron microscope. Light scattering (DLS) and ζ potentials were performed on BROOKHAVEN ZETAPALS/BI-200SM. The samples were prepared by dropping the solution onto silicon wafer and then air-dried. Fluorescence microscopy images were recorded by a confocal laser scanning microscope (A1R+, Nikon, Japan). The in vivo imaging of the compounds in the injected nude mice was performed via the IVIS Lumina II monitored by using the Cy5.5 mode.

Theoretical calculations

The density functional theory (DFT) calculations were implemented using the Gaussian 16 program.[1] The geometry optimizations and frequencies of the **TP-3PY** were

calculated in B3LYP[2] functional employing a basis set of 6-31G(d)[3].

Cell culture

HeLa cells were incubated in Dulbecco's modified eagle medium (DMEM) supplemented with 10% fetal bovine serum (FBS) and 1% penicillin/streptomycin. The cells were harvested from the cell culture medium by incubating in a trypsin solution for 2 min. After centrifugation for 2 min at 900 rpm, the supernatant was discarded. A protion of serum-supplemented medium (3 ml) was added to neutralize the residual trypsin. Then, the cells were resuspended in serum-supplemented medium and cultured at 37 °C and 5% CO_2. The cells were sub-cultured when the density reached 80%. For fluorescence confocal microscopy, the cells were incubated for 10 hours at 37 °C after treating with samples in medium. Next, Mito Tracker Green and Lyso Tracker Green cocultured with the cells at 37 °C for 30 min to stain the mitochondria and lysosomes. Then, cells were washed 3 times with PBS buffer before imaging by confocal laser scanning microscopy. The excitation wavelengths for the green and red channels were all 405 nm, and the emission wavelength ranges for the green and red channels were 500-545 nm and 650-750 nm, respectively.

Cytotoxicity experiments

HeLa cells were incubated by using DMEM supplemented with 10% FBS and 1% penicillin/streptomycin in a humidified incubator with 5% CO_2. Hela cells were seeded at a density of 5×10^4 cells per well into a 96-well plate. After adherence, the cells were treated with **TP-3PY**, **TP-3PY**⊂CB[8] and **TP-3PY**⊂CB[7] of different concentrations ranging from 0 to 25 μM. After incubation for 24 hours, the culture medium was replaced with fresh medium. The relative cellular viability was determined by the CCK-8 assay according to instruction. Absorbance of the plate was then read by a microplate reader at a wavelength of 450 nm. Untreated cells were employed as a control. All experiments were conducted with four replicates. The cell viability was calculated according to the equation: $CV = A/A_0 \times 100\%$, where A is the

absorbance of the experimental group and A_0 is the absorbance of the control group, respectively.

2. Synthesis and characterization of compounds

2.1 Synthesis of TP-3PY

Scheme S1. Synthesis routes of TP-3PY.

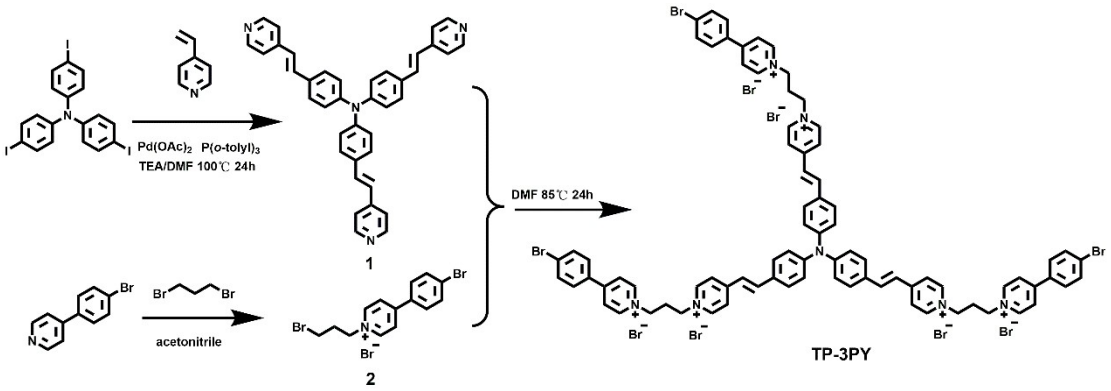

Synthesis of Tris[*p*-(4-pyridylvinyl)]amine (1).

Compound **1** was synthesized according to the literature.[4] Compound tris(4-iodophenyl)]amine (3.115 g, 5 mmol), 4-vinylpyridine (3 g, 3.12 ml, 29 mmol), $Pd(OAc)_2$ (33 mg, 0.15 mmol), tri-*o*-tolylphosphine (93 mg, 0.3 mmol), triethylamine (5 ml) and N'N-Dimethylformamide (35 ml) were added to a stirred round-bottom flask and degassed with nitrogen. The reaction mixture was stirred under reflux at 100 ℃ for 24 hours. After cooling to room temperature, the mixture was poured into water and got orange solid. Then the mixture was filtered off and the solid was washed by water for several times. And then the solid was dried under vacuum and purified by chromatography to obtain compound **1** as an orange powder (1.86 g, yield 67%). ^{1}H NMR (400 MHz, DMSO-d_6): δ 8.53 (d, J = 6.0 Hz, 6H), 7.63 (d, J = 8.8 Hz, 6H), 7.53 (t, 9H), 7.16 (d, J = 16.4 Hz, 3H), 7.10 (d, J = 8.8 Hz, 6H).

Synthesis of TP-3PY.

Compound **1** (33 mg, 0.06 mmol) and compound **2**[5] (91mg, 0.21 mmol) was added to a stirred round-bottom flask in DMF (10 ml). The mixture was stirred under reflux at 85 ℃ for 24 hours. After cooling to room temperature, the mixture was dropped into ethyl ether and got red solid. The solvent was removed by filtration and the solid was washed by ethyl ether for several times. And then the solid was purified by chromatography after ion exchange to PF_6^- with MeCN/0-2% NH_4PF_6 as eluent. Finally, the ion of compound was exchanged to Br^- and dried under vacuum to obtain compound **TP-3PY** as a red powder (19.9 mg, yield 18%). ^{1}H NMR (400 MHz, CD_3OD-d_4): δ9.09 (d, J = 6.8 Hz, 6H), 8.88 (d, J = 6.8 Hz, 6H), 8.46 (d, J = 6.8 Hz, 6H), 8.19 (d, *J* = 6.8 Hz, 6H), 8.02-7.92 (m, 9H), 7.88-7.73 (dd, 12H), 7.39 (d, *J* = 16.4 Hz, 3H), 7.22 (d, *J* = 8.8 Hz, 6H), 4.82-4.72 (m, 12H), 2.89-2.79 (m, 6H). ^{13}C NMR (400 MHz, DMSO-d_6): δ145.11, 144.32, 132.69, 130.12, 126.38, 124.50, 123.61, 56.88, 56.46, 31.34. ESI-HRMS *m*/*z* for **TP-3PY** ($C_{81}H_{72}N_7Br_9$) calcd. $[M\text{-}3Br^-]^{3+}/3$: 540.6957, found: 540.6971.

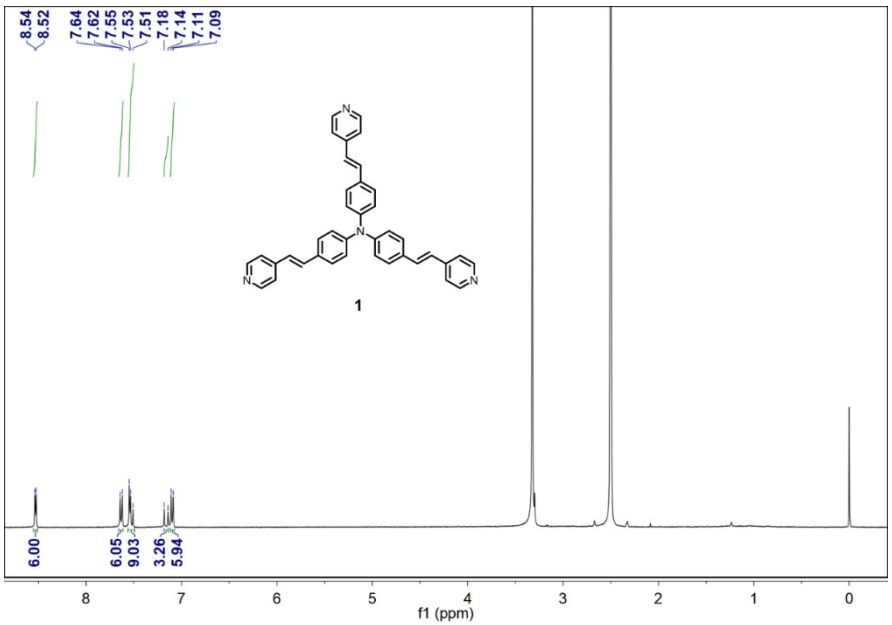

Figure S1. ^{1}H NMR spectrum of **1** (400 MHz, DMSO-d_6, 298 K).

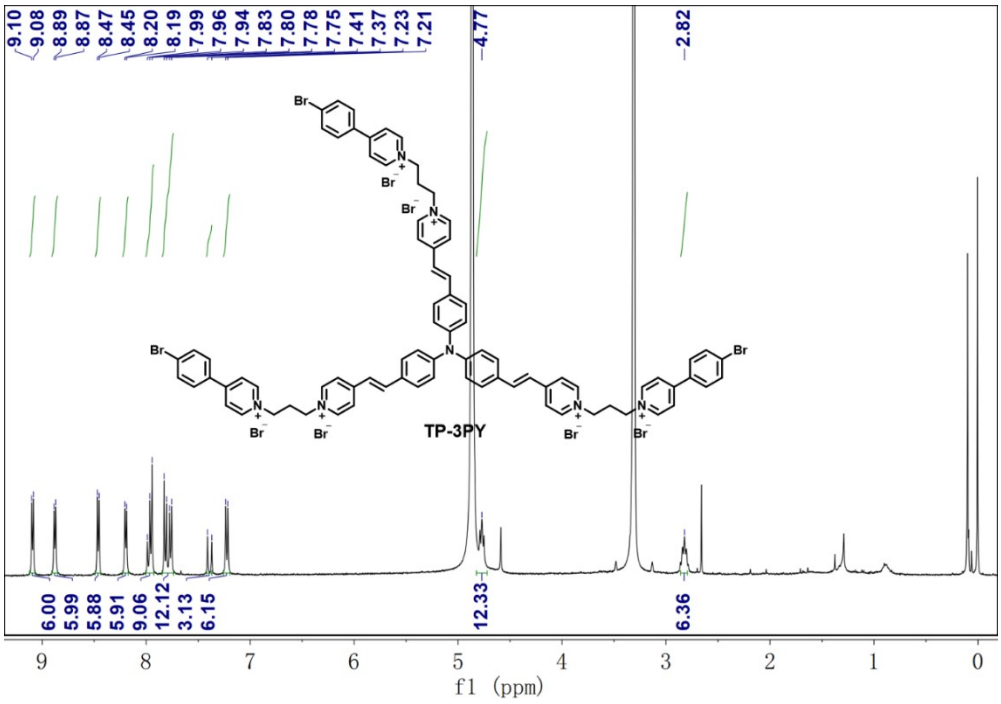

Figure S2. ^{1}H NMR spectrum of **TP-3PY** (400 MHz, CD_3OD-d_4, 298 K).

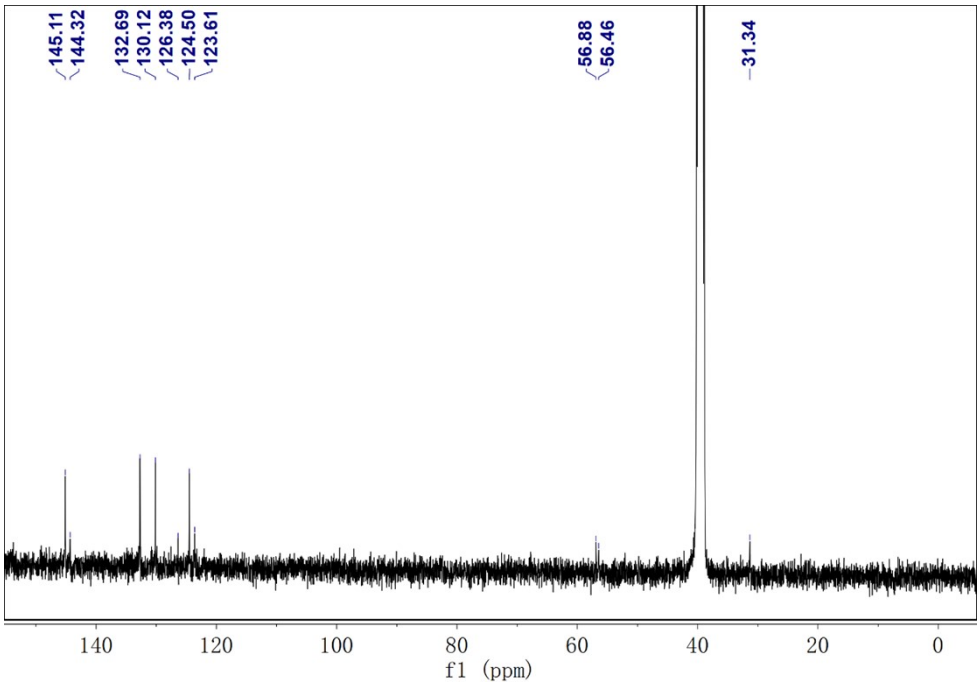

Figure S3. ^{13}C NMR spectrum of **TP-3PY** (100 MHz, DMSO-d_6, 298 K).

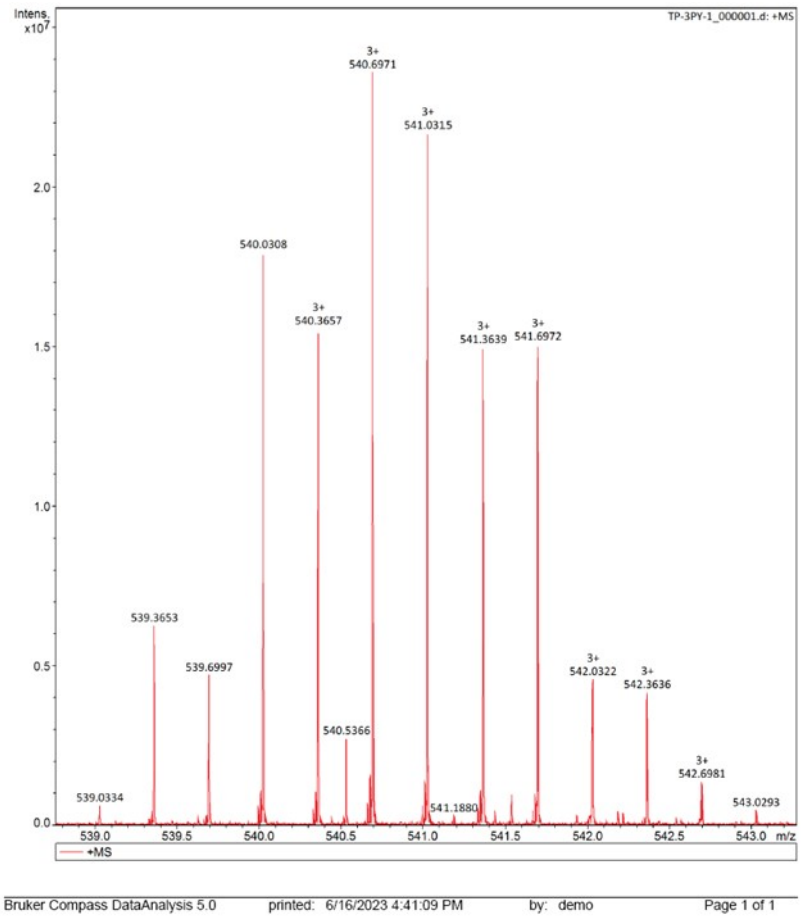

Figure S4. ESI-HRMS *m/z* for **TP-3PY** ($C_{81}H_{72}N_7Br_9$) calcd. $[M\text{-}3Br^-]^{3+}/3$: 540.6957, found: 540.6971.

2.2 Synthesis of compound A-PY

Scheme S2. Synthesis route of compound A-PY.

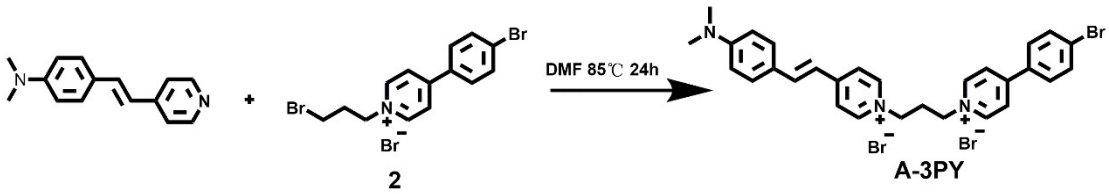

Sythesis of compound A-PY.

4-[4-(dimethylamino)styryl]pyridine (112 mg, 0.5 mmol) and compound **2** (216 mg, 0.5 mmol) was added to a stirred round-bottom flask in DMF (20 ml). The mixture was stirred under reflux at 85 ℃ for 24 hours. After cooling to room temperature, the mixture was dropped into ethyl ether and got red solid. The solvent was removed by filtration and the solid was washed by ethyl ether for several times. And then the solid was dried under vacuum to obtain compound **A-PY** as a red powder (152 mg, yield 46%). ^{1}H NMR (400 MHz, DMSO-d_6): δ 9.12 (d, J = 6.8 Hz, 2H), 8.76 (d, J = 6.8 Hz, 2H), 8.58 (d, J = 6.8 Hz, 2H), 8.11-8.02 (m, 4H), 7.94 (d, J = 12.0 Hz, 1H), 7.87 (d, J = 8.4 Hz, 2H), 7.59 (d, J = 8.8 Hz, 2H), 7.87 (d, J = 16.0 Hz, 1H), 6.79 (d, J = 8.8 Hz, 2H), 4.70 (t, 2H), 4.55 (t, 2H), 3.03 (t, 6H), 2.64 (t, 2H). ^{13}C NMR (400 MHz, DMSO-d_6): δ 154.54, 154.20, 152.47, 145.59, 144.08, 142.99, 133.16, 133.10, 130.75, 130.62, 126.84, 124.99, 122.89, 117.51, 112.43, 57.36, 56.43, 31.83. MALDI-TOF-HRMS *m/z* for **A-PY** ($C_{29}H_{30}N_3Br_3$): calcd. $[M\text{-}2Br^-]^{2+}/2$: 249.5806, found:249.5809.

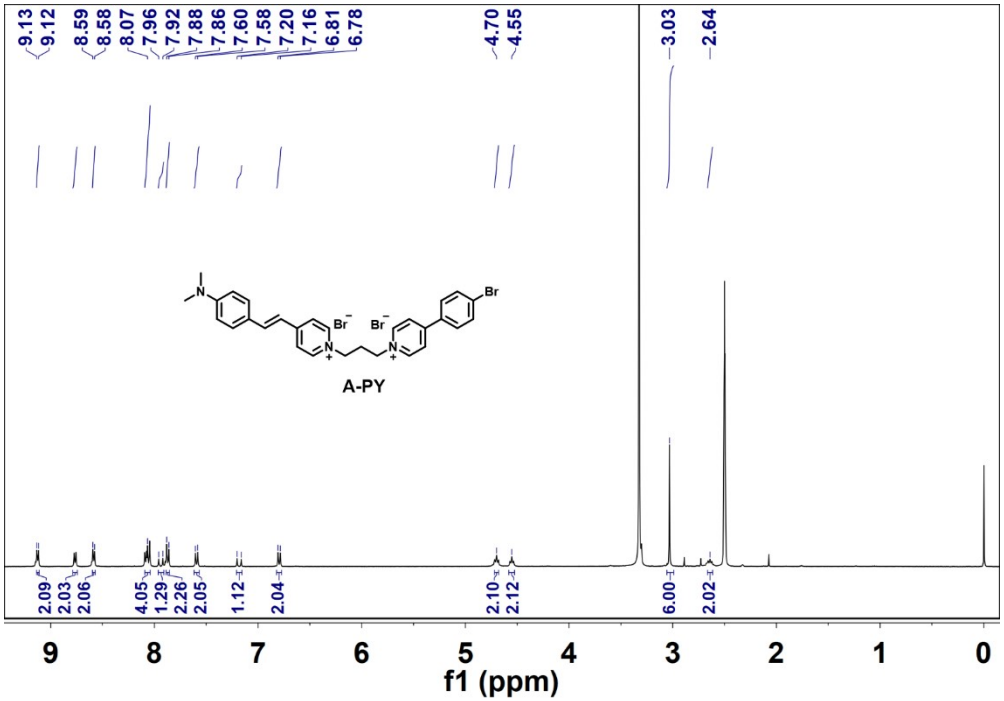

Figure S5. ^{1}H NMR spectrum of **A-PY** (400 MHz, DMSO-d_6, 298 K).

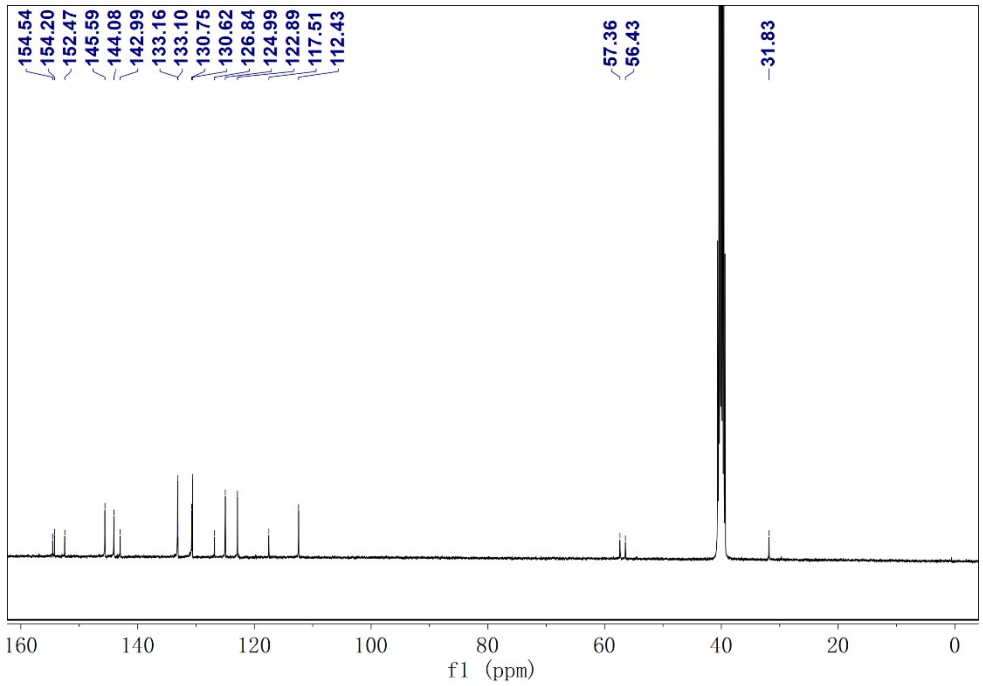

Figure S6. ^{13}C NMR spectrum of **A-PY** (100 MHz, DMSO-d_6, 298 K).

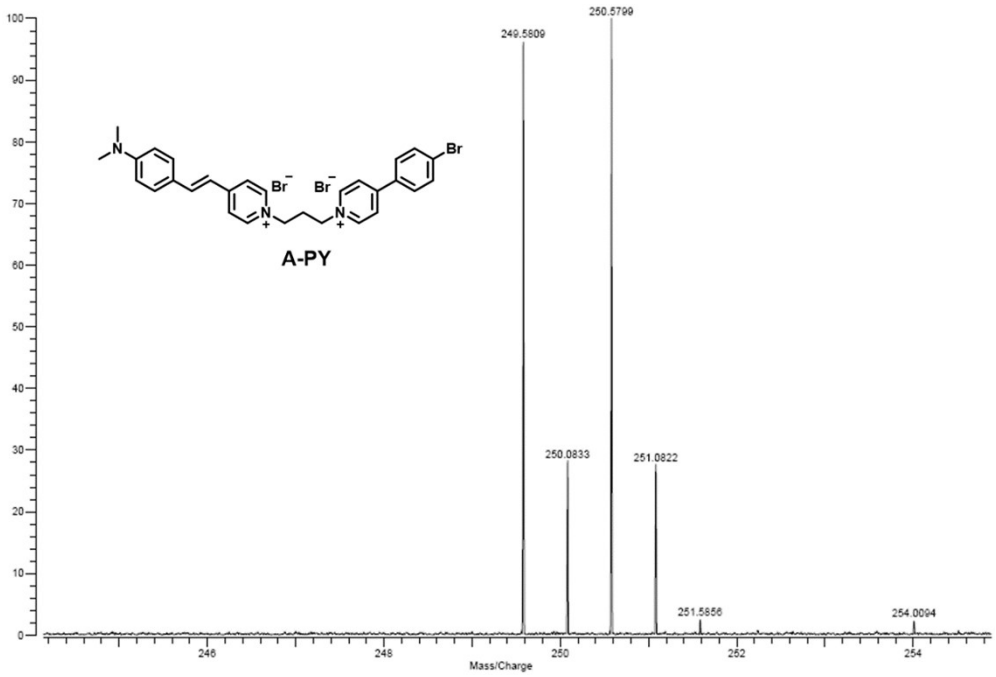

Figure S7. MALDI-TOF-HRMS *m/z* for **A-PY** ($C_{29}H_{30}N_3Br_3$) calcd. $[M\text{-}2Br^-]^{2+}/2$: 249.5806, found: 249.5809.

3. Characterization of Suparmolecular Assembly

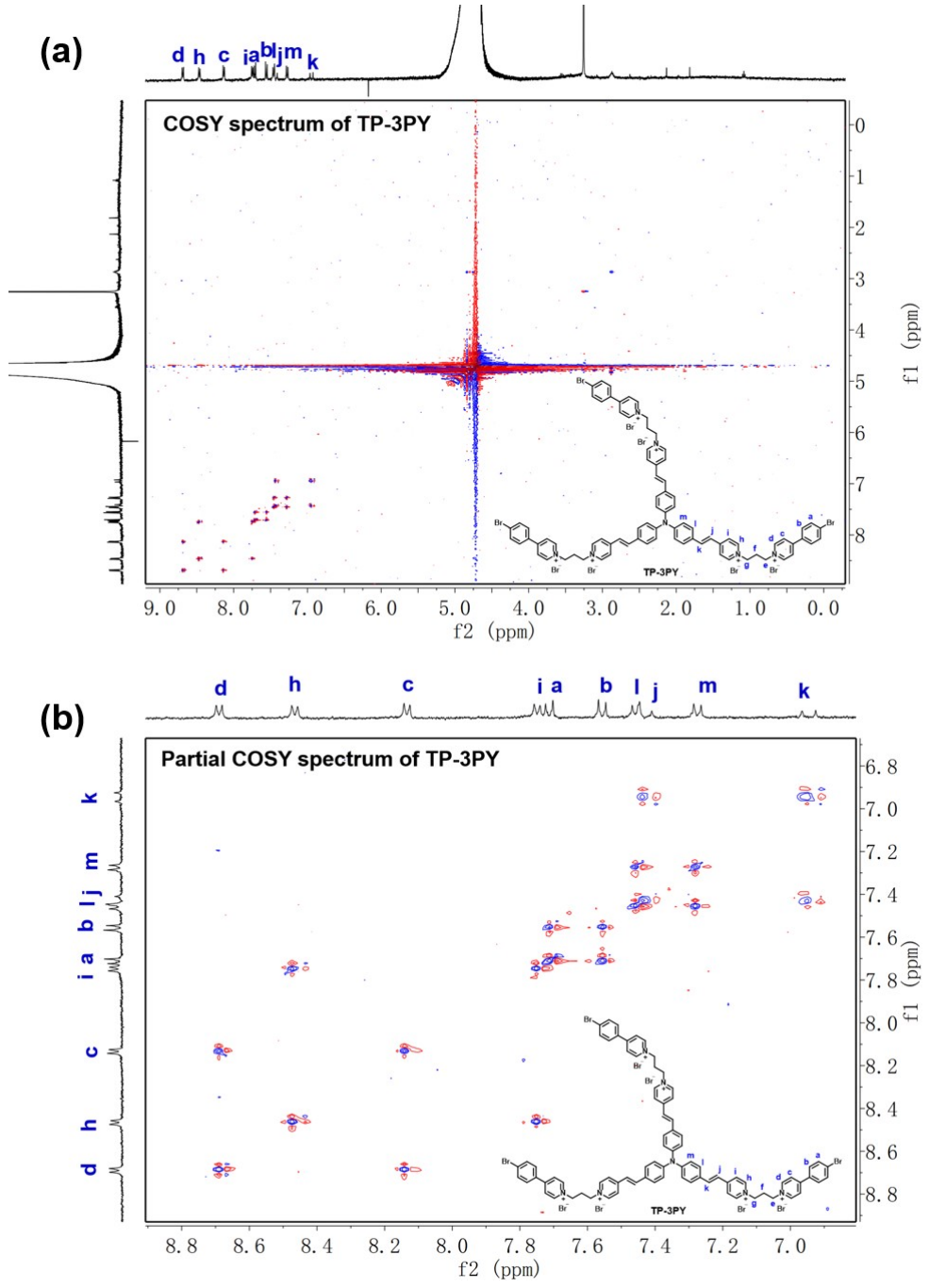

Figure S8. 2D ^{1}H-^{1}H COSY NMR spectra of **TP-3PY** (3×10^{-4} M, 400 MHz, D_2O, 298 K).

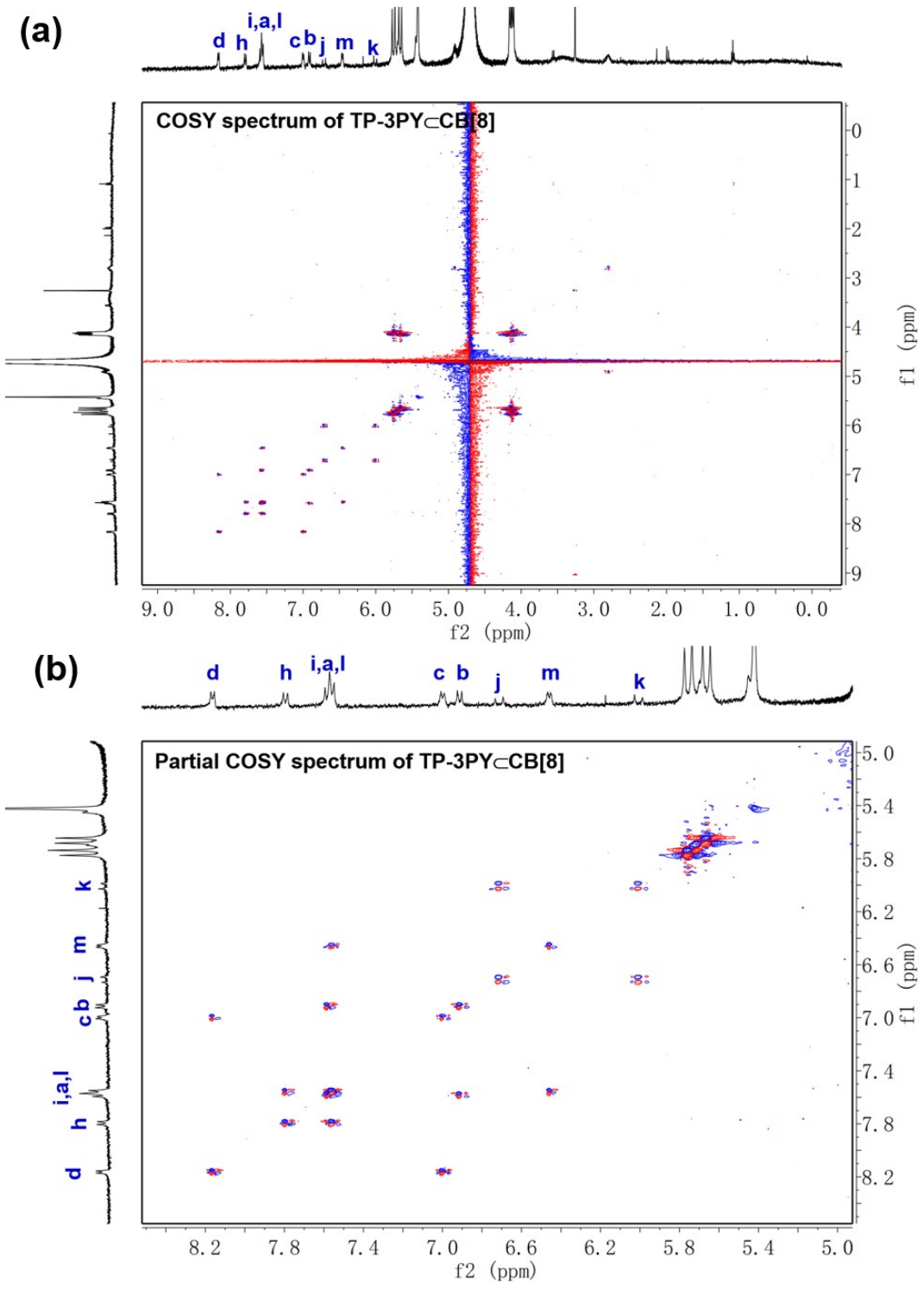

Figure S9. 2D ^{1}H-^{1}H COSY NMR spectrum of **TP-3PY**⊂CB[8] ([**TP-3PY**] = 3 × 10^{-5} M, [CB8] = 9 × 10^{-5} M, 400 MHz, D_2O, 298 K).

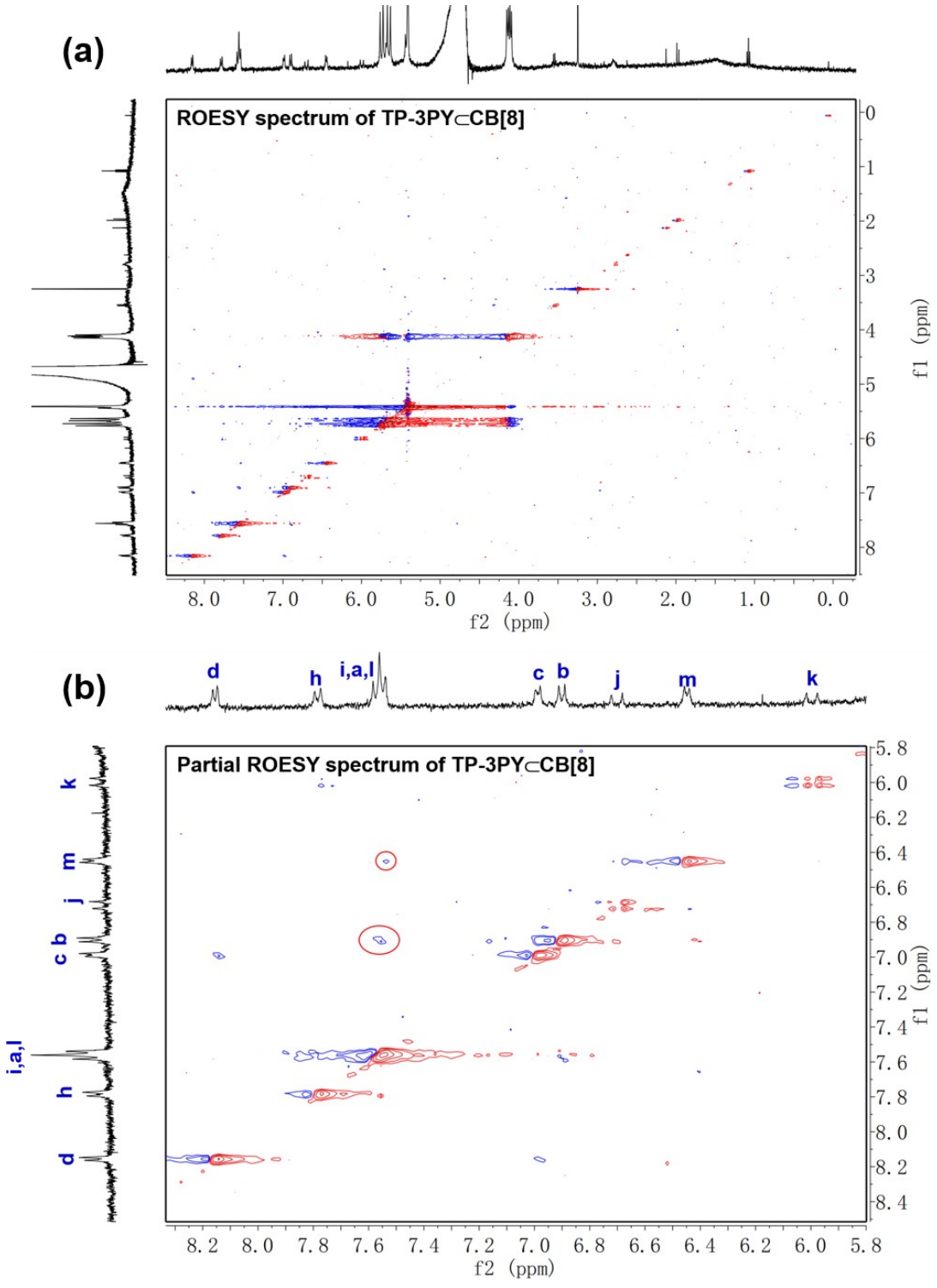

Figure S10. 2D ROESY spectra of **TP-3PY**⊂CB[8] ([**TP-3PY**] = 1 × 10^{-4} M, [CB[8]] = 3 × 10^{-4} M, 400 MHz, D_2O, 298 K).

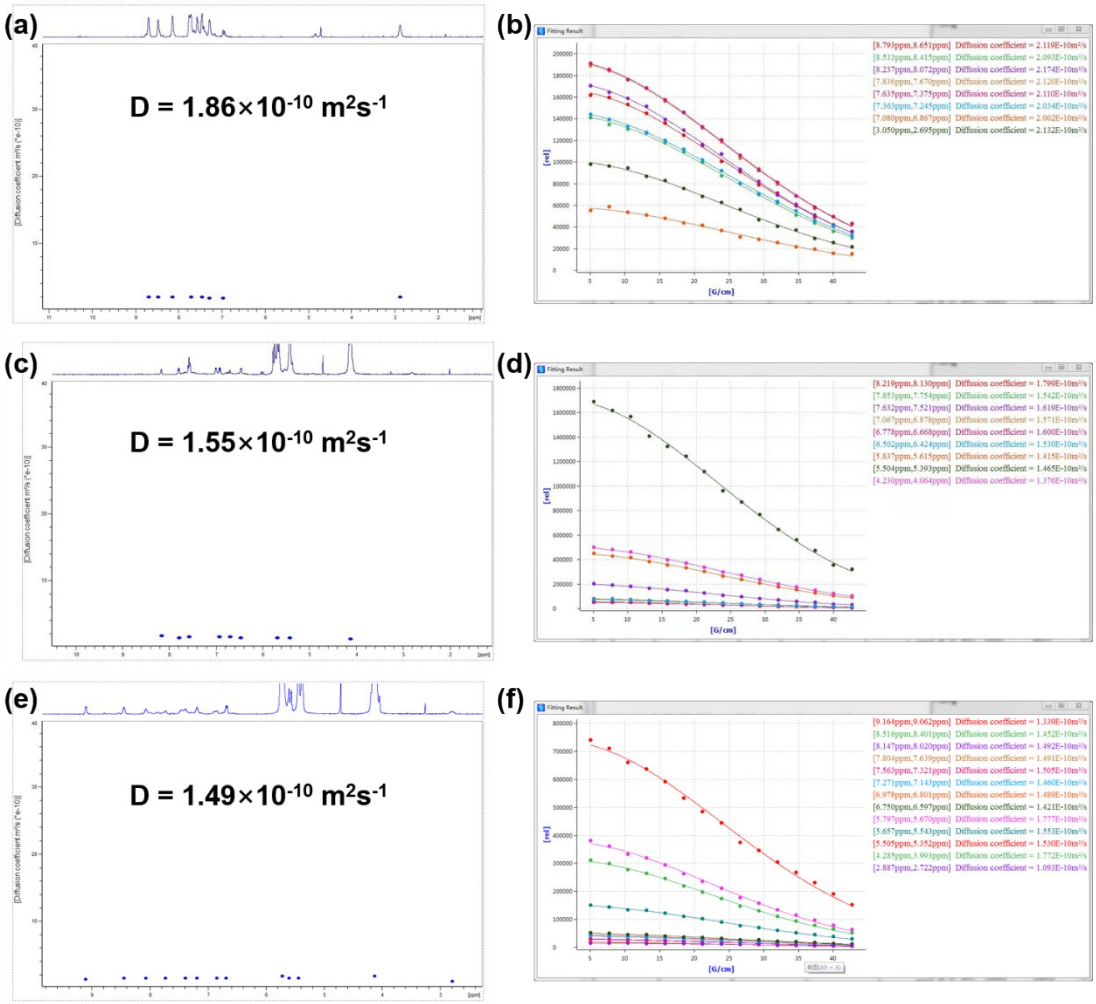

Figure S11. 2D DOSY spectra of (a) **TP-3PY**, (c) **TP-3PY**⊂CB[8], (e) **TP-3PY**⊂CB[7]. Diffusion coefficient of (b) **TP-3PY**, (d) **TP-3PY**⊂CB[8], (f) **TP-3PY**⊂CB[7] ([**TP-3PY**] = 1 × 10^{-4} M, [CB[8]] = 3 × 10^{-4} M, [CB[7]] = 6 × 10^{-4} M, 400 MHz, D_2O, 298 K).

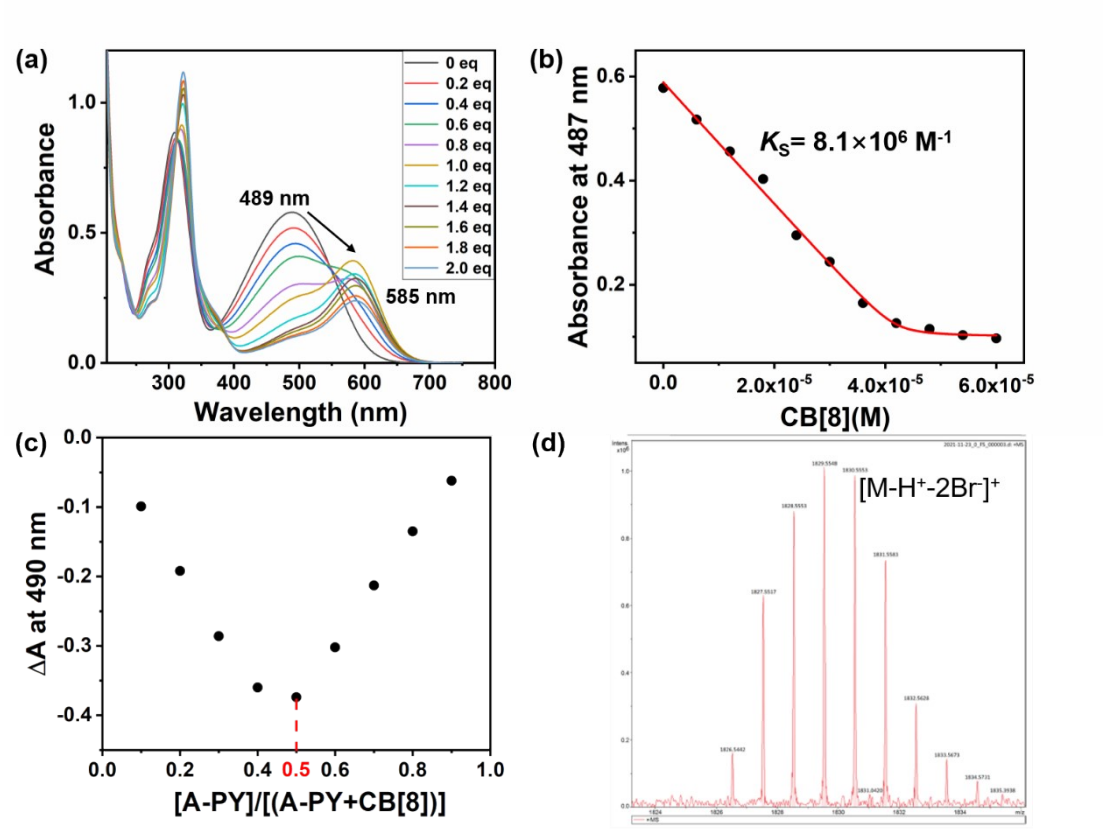

Figure S12. (a) UV-vis absorption spectra of **A-PY** (3×10^{-5} M) with different concentration of CB[8] (0 μM, 6 μM, 12 μM, 18 μM, 24 μM, 30 μM, 36 μM, 42 μM, 48 μM, 54 μM, 60 μM) in aqueous solution at 298 K. (b)The nonlinear least-squares analysis of the variation of absorbance with the concentration CB[8] to calculate the binding constant from the corresponding absorbance in (a). (c) Job's experiment for **A-PY** upon complexation with CB[8] in aqueous solution at 298 K. Absorbance changes of **A-PY** recorded at 490 nm were used to analyze the binding ratio. The total concentration of host and guest is constant ([**A-PY**] + [CB[8]] = 6.25×10^{-5} M). (d) MALDI-TOF-HRMS of **A-PY**⊂CB[8] ($C_{77}H_{78}Br_3N_{35}O_{16}$) calcd. $[M-H^+-2Br^-]^+$:1826.5460, found:1826.5442.

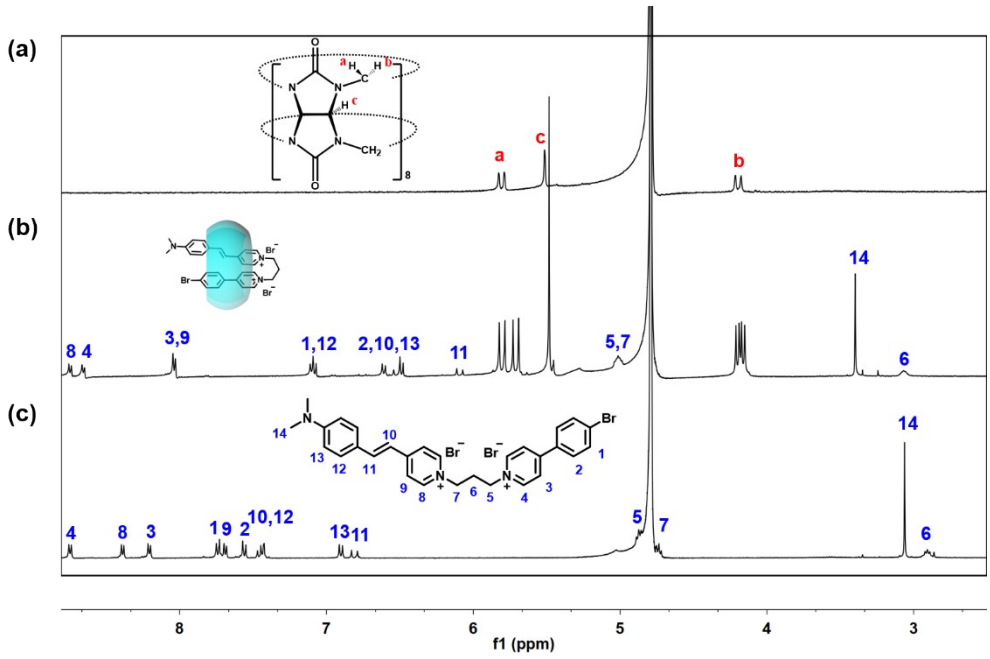

Figure S13. ^{1}H NMR spectra of (a) CB[8], (b) **A-PY**⊂CB[8] and (c) **A-PY** ([CB[8]] = [**A-PY**] = 10^{-3} M, 400 MHz, D_2O, 298 K).

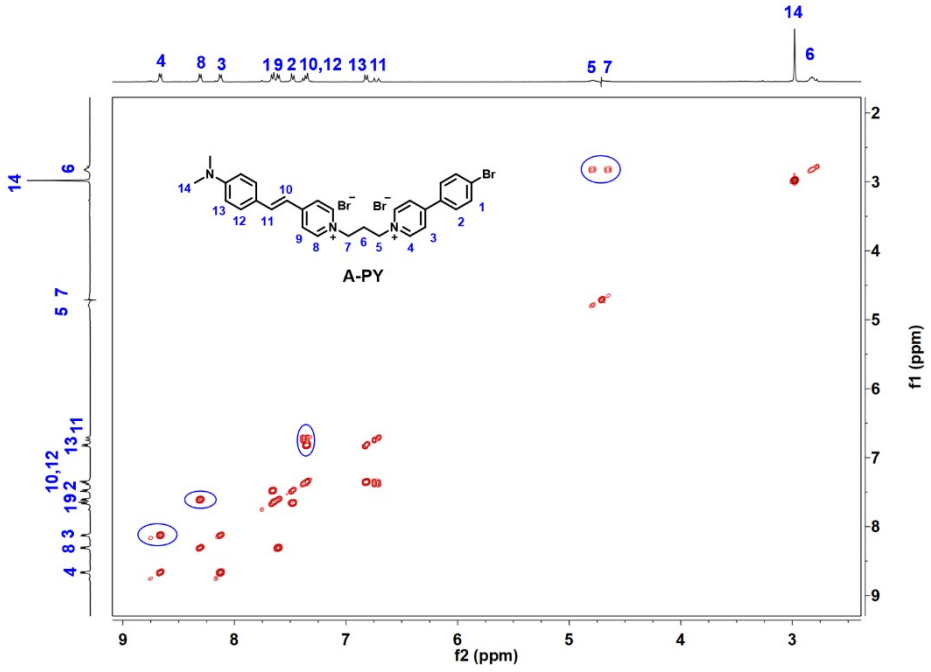

Figure S14. 2D ^{1}H-^{1}H COSY NMR spectrum of **A-PY** ([**A-PY**] = 10^{-3} M, 400 MHz, D_2O, 298 K).

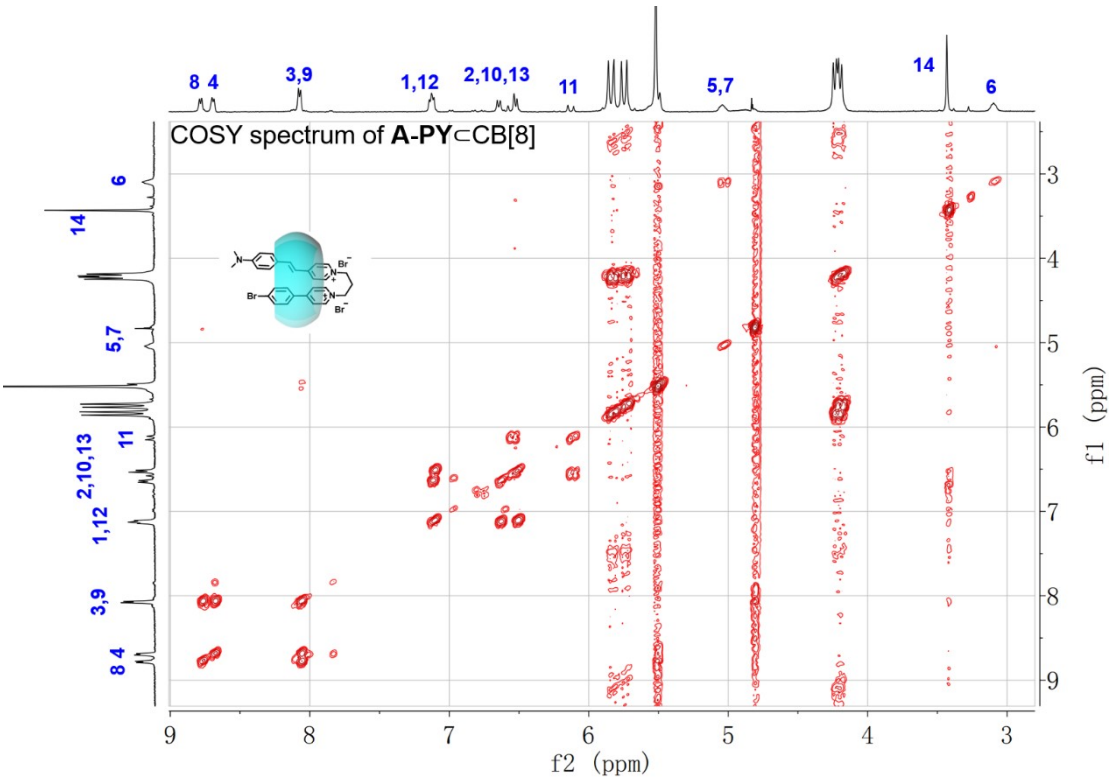

Figure S15. 2D ^{1}H-^{1}H COSY NMR spectrum of **A-PY**⊂CB[8] ([CB[8]] = [**A-PY**] = 10^{-3} M, 400 MHz, D_2O, 298 K).

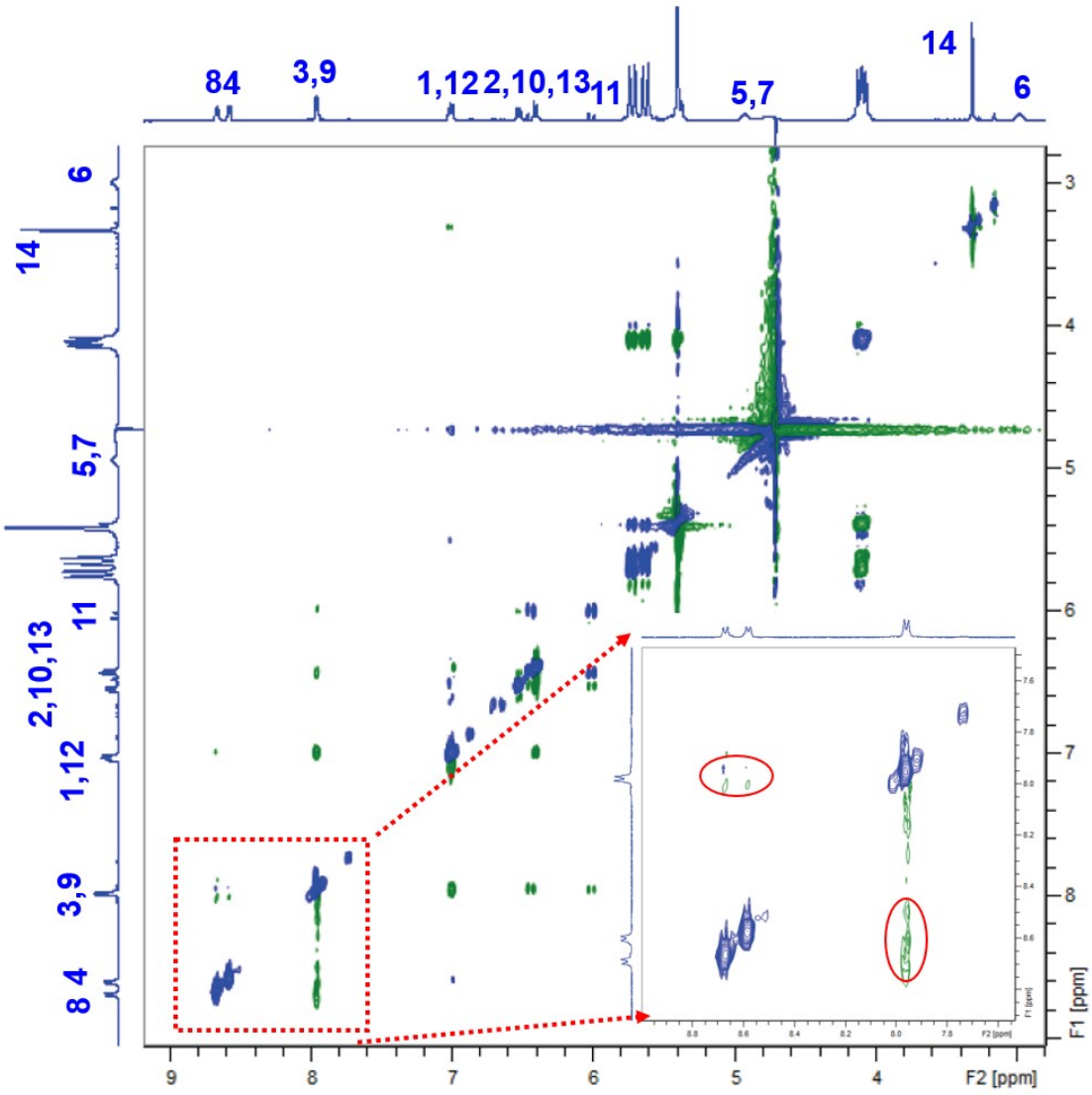

Figure S16. 2D ^{1}H-^{1}H ROESY NMR spectrum of **A-PY**⊂CB[8] (CB[8] = [**A-PY**] = 10^{-3} M, 400 MHz, D_2O, 298 K).

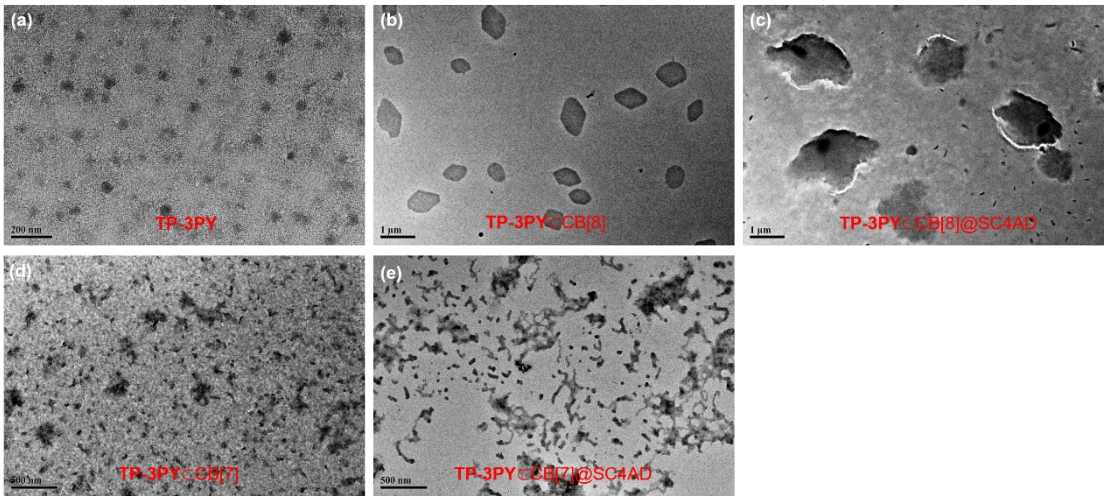

Figure S17. TEM spectra of (a) **TP-3PY**, (b) **TP-3PY**⊂CB[8], (c) **TP-3PY**⊂CB[8]@SC4AD, (d) **TP-3PY**⊂CB[7] and (e) **TP-3PY**⊂CB[7]@SC4AD.

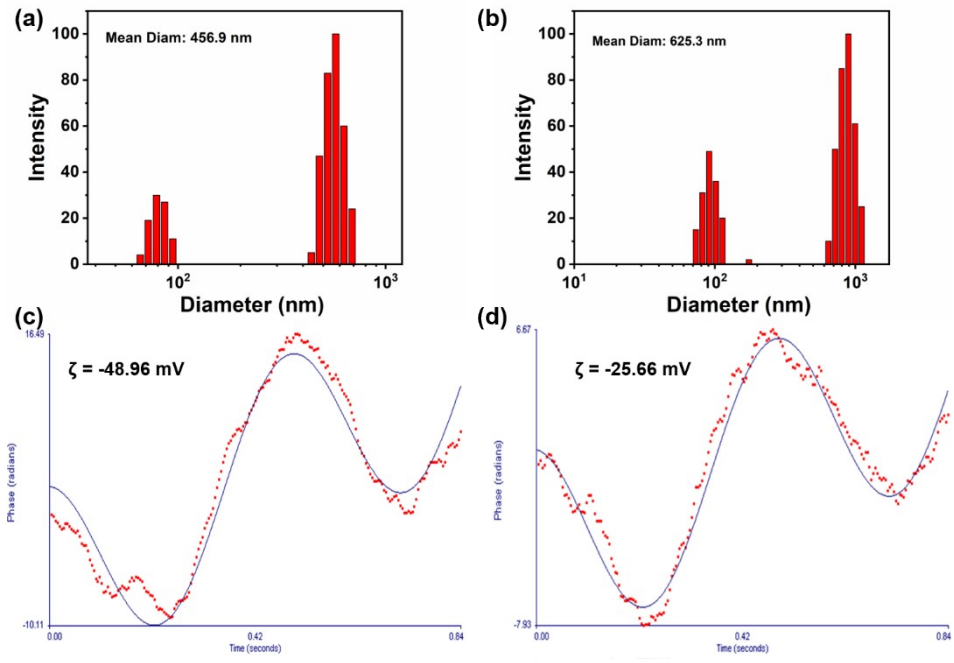

Figure S18. Dynamic light scattering data (DLS) data of (a) **TP-3PY**⊂CB[8]@SC4AD and (b) **TP-3PY**⊂CB[7]@SC4AD. Zeta potentials of (c) **TP-3PY**⊂CB[8]@SC4AD and (d) **TP-3PY**⊂CB[7]@SC4AD.

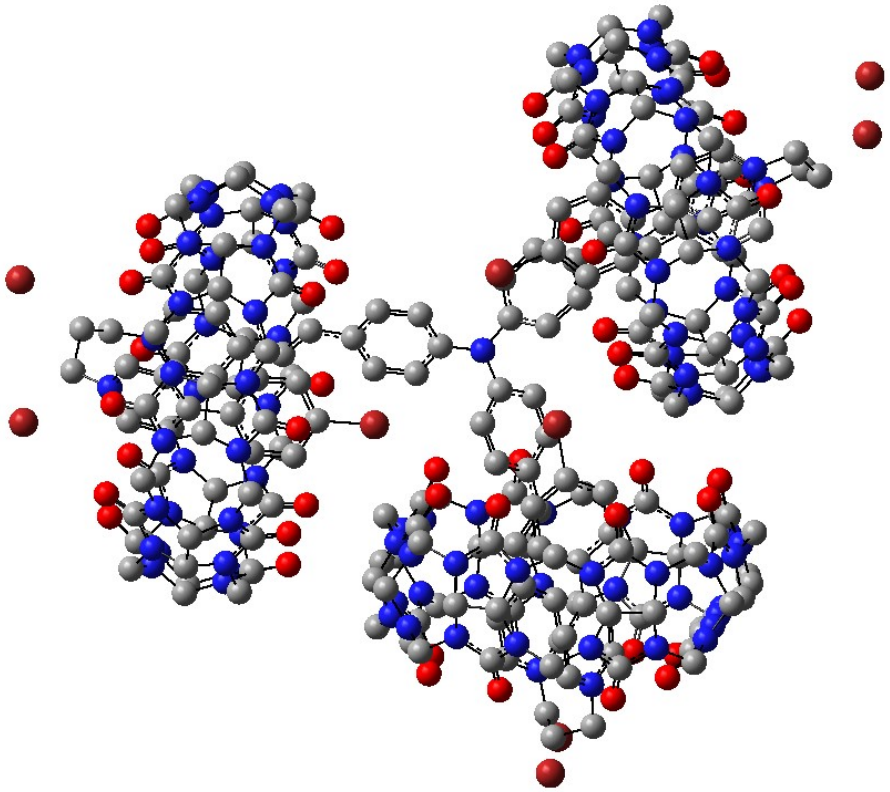

Figure S19. Simulated structure of supramolecular assembly **TP-3PY**⊂CB[8].

4. Photophysical properties

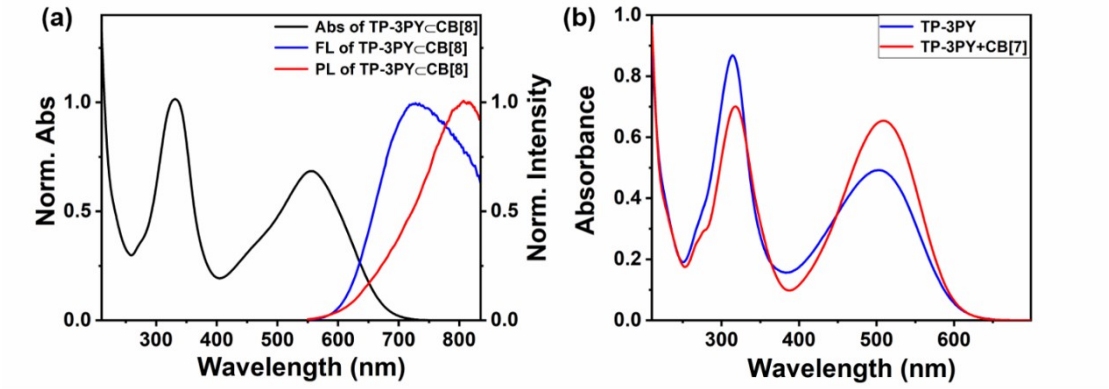

Figure S20. (a) UV/vis absorption, fluorescence and phosphorescence spectra of **TP-3PY**⊂CB[8] ([**TP-3PY**] = 2 × 10^{-5} M, CB[8] = 6 × 10^{-5} M, λ_{ex} = 509 nm). (b) UV/vis

absorption spectra of **TP-3PY** and **TP-3PY**⊂CB[7] ([**TP-3PY**] = 10^{-5} M, CB[7] = 6 × 10^{-5} M).

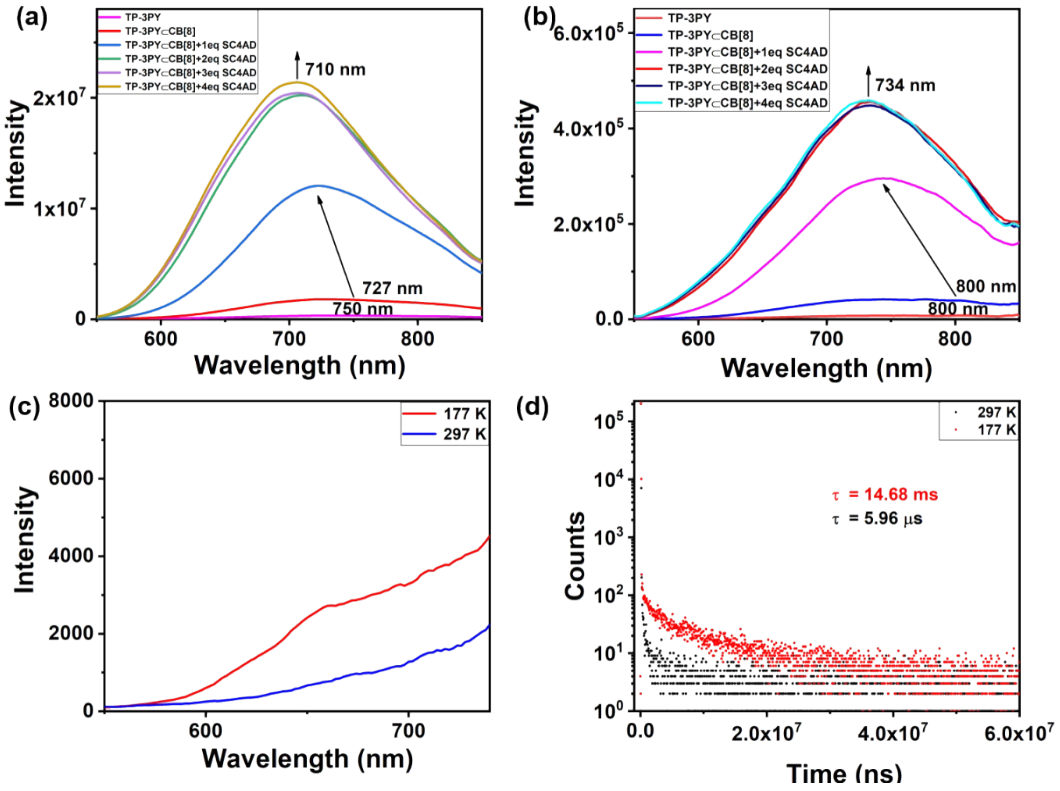

Figure S21. (a) Fluorescence emission spectra and (b) phosphorescence emission spectra (delayed 50 μs) of **TP-3PY**⊂CB[8] ([**TP-3PY**] = 2 × 10^{-5} M, CB[8] = 6 × 10^{-5} M, λ_{ex} = 509 nm) with different concentration of SC4AD (0 μM, 20 μM, 40 μM, 60 μM and 80 μM). (c) Phosphorescence emission spectra (delayed 50 μs) and (d) time-resolved PL decay curves of **TP-3PY**⊂CB[8]@SC4AD at different temperature ([**TP-3PY**] = 2 × 10^{-5} M, CB[8] = 6 × 10^{-5} M, [SC4AD] = 4 × 10^{-5} M, λ_{ex} = 509 nm).

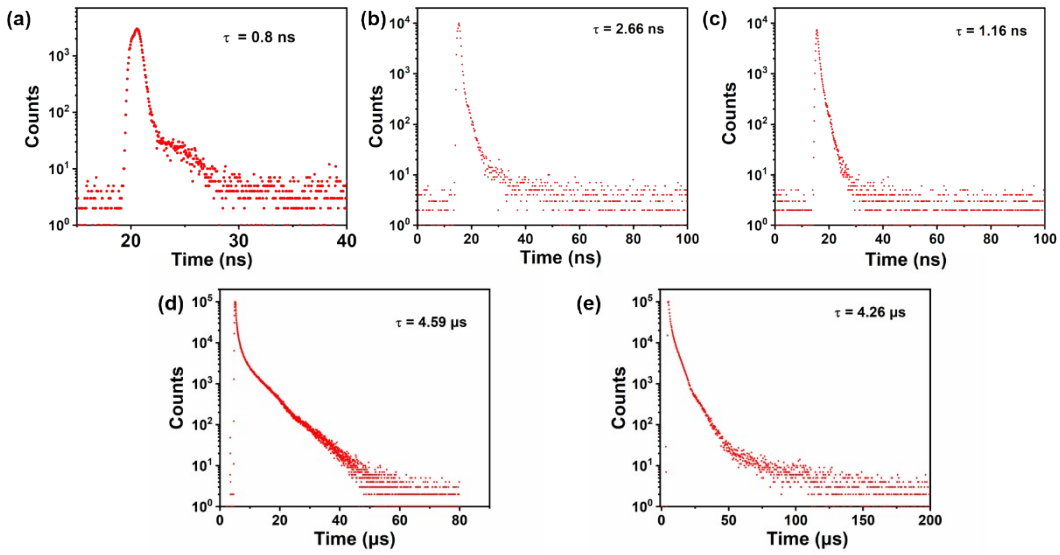

Figure S22. Time-resolved FL decay curves of (a) **TP-3PY** (750 nm), (b) **TP-3PY**⊂CB[8] (730 nm) and (c) **TP-3PY**⊂CB[8]@SC4AD (710 nm). Time-resolved PL decay curves of (d) **TP-3PY**⊂CB[8] (800 nm) and (e) **TP-3PY**⊂CB[8]@SC4AD (730 nm) ([**TP-3PY**] = 2 × 10^{-5} M, [CB[8]] = 6 × 10^{-5} M, [SC4AD] = 4 × 10^{-5} M, λ_{ex} = 509 nm).

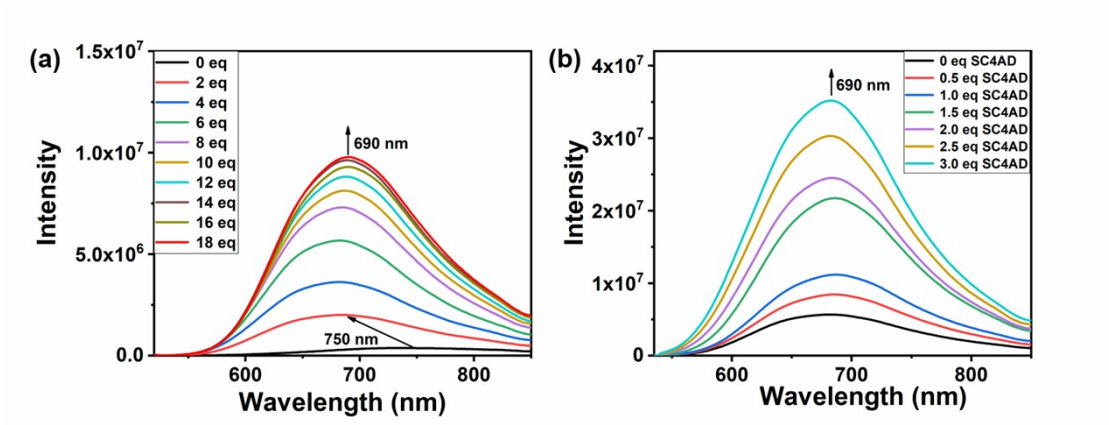

Figure S23. Fluorescence emission spectra of (a) **TP-3PY** ([**TP-3PY**] = 2 × 10^{-5} M, λ_{ex} = 509 nm) with different concentration of CB[7] (0-360 μM). (b)**TP-3PY**⊂CB[7] ([**TP-3PY**] = 2 × 10^{-5} M, CB[7] = 12 × 10^{-5} M, λ_{ex} = 509 nm) with different

concentration of SC4AD (0 μM, 10 μM, 20 μM, 30 Mm, 40 μM, 50 μM and 60 μM).

compound	λ_{abs} (nm)	λ_{FL} (nm)	λ_{PL} (nm)
TP-3PY	315/509	750	NA
TP-3PY⊂CB[8]	332/556	727	800
TP-3PY⊂CB[8]@SC4AD	NA	710	734
TP-3PY⊂CB[7]	318/514	690	NA
TP-3PY⊂CB[7]@SC4AD	NA	690	NA
1	305/440	390/530	NA
1⊂CB[8]	495	390/530	720
1⊂CB[8]@SC4AD	495	NA	670
2	300/440	390/620	NA
2⊂CB[8]	510	390/620	800
2⊂CB[8]@SC4AD	510	NA	680
3	472	572	NA
3⊂CB[8]	543	714	NA
3⊂CB[7]	506	635	NA

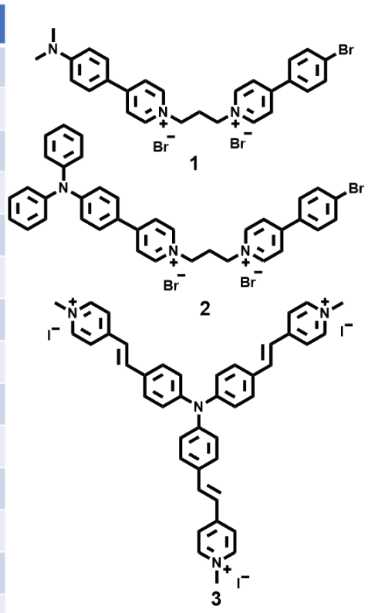

Figure S24. Summary of optical properties of the compounds. The optical properties of compound **1**[6], **2**[6] and **3**[7] were accepted from the reported literatures. λ_{abs}, λ_{FL} and λ_{PL} are maxima of absorption, FL and PL respectively. NA: not accept.

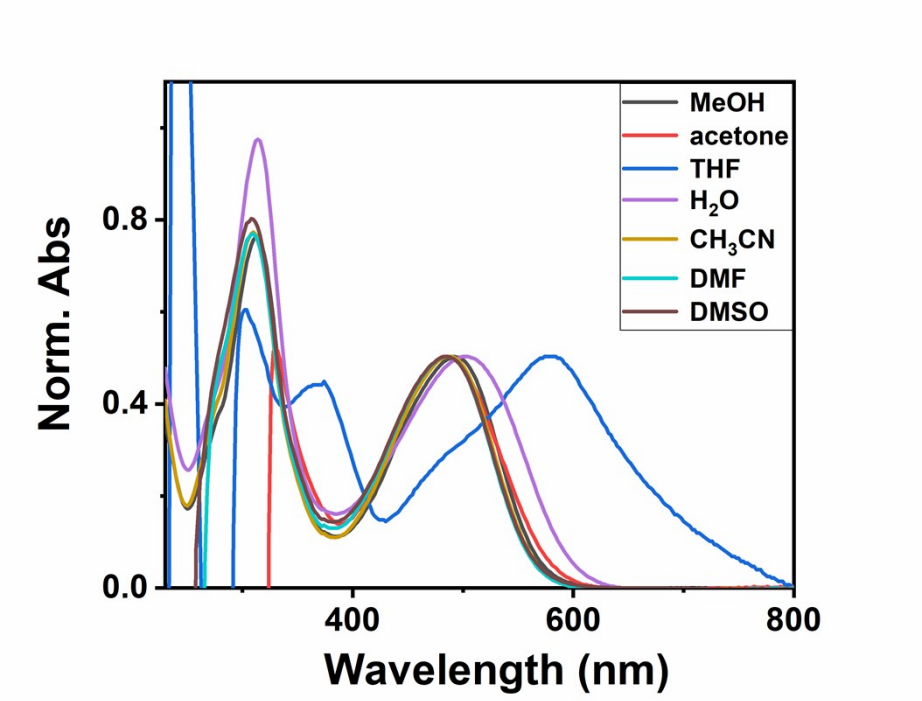

Figure S25. The normalized absorbance of **TP-3PY** in different solvents.

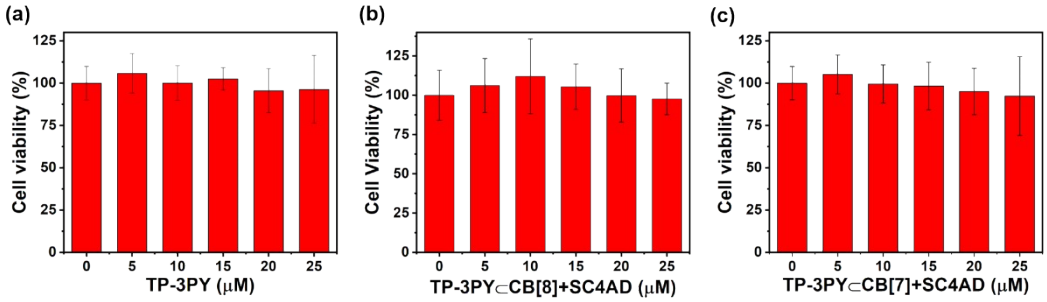

Figure S26. Viabilities of HeLa cells upon incubation with different concentrations of (a) **TP-3PY**, (b) **TP-3PY**⊂CB[8]@SC4AD and (c) **TP-3PY**⊂CB[7]@SC4AD.

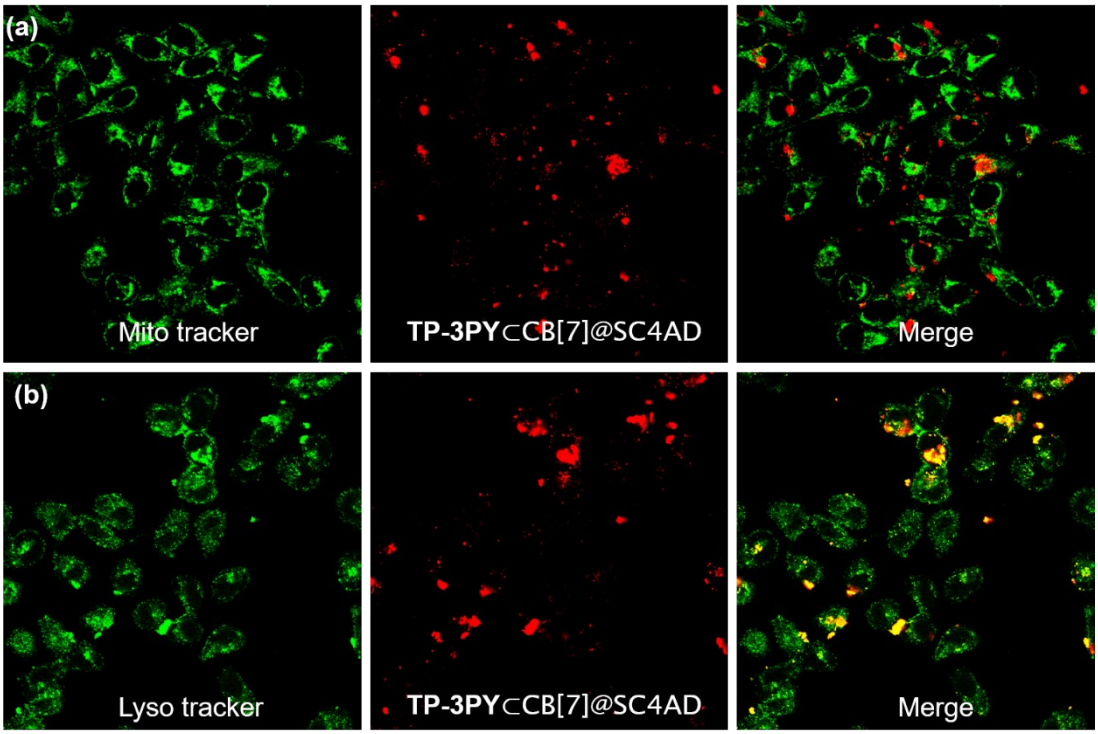

Figure S27. CLMS images of HeLa cells co-stained with **TP-3PY**⊂CB[7]@SC4AD ([**TP-3PY**] = 2 × 10^{-6} M, [CB[7]] = 12 × 10^{-6} M], [SC4AD] = 6 × 10^{-6} M) and (a) Mito Tracker Green, (b) Lyso Tracker Green, respectively.

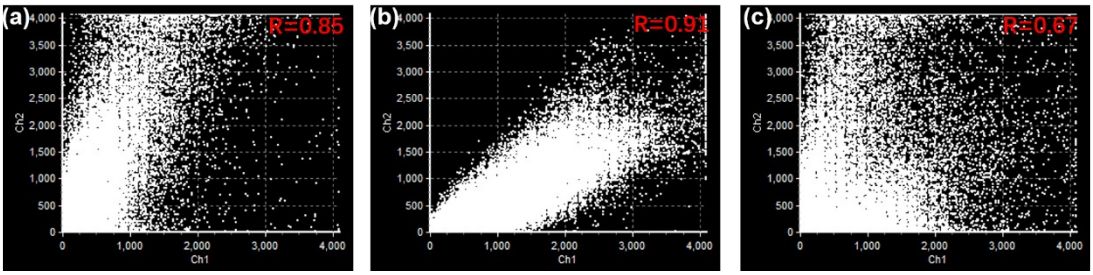

Figure S28. Confocal laser Pearson's correlation coefficient for lysosome co-localization images of **TP-3PY**, **TP-3PY**⊂CB[8]@SC4AD and **TP-3PY**⊂CB[7]@SC4AD, respectively.

References

[1] M. J. Frisch, G. W. Trucks, H. B. Schlegel, G. E. Scuseria, M. A. Robb, J. R. Cheeseman, G. Scalmani, V. Barone, G. A. Petersson, H. Nakatsuji, X. Li, M. Caricato, A. V. Marenich, J. Bloino, B. G. Janesko, R. Gomperts, B. Mennucci, H. P. Hratchian, J. V. Ortiz, A. F. Izmaylov, J. L. Sonnenberg, D. Williams-Young, F. Ding, F. Lipparini, F. Egidi, J. Goings, B. Peng, A. Petrone, T. Henderson, D. Ranasinghe, V. G. Zakrzewski, J. Gao, N. Rega, G. Zheng, W. Liang, M. Hada, M. Ehara, K. Toyota, R. Fukuda, J. Hasegawa, M. Ishida, T. Nakajima, Y. Honda, O. Kitao, H. Nakai, T. Vreven, K. Throssell, J. A. Montgomery, Jr., J. E. Peralta, F. Ogliaro, M. J. Bearpark, J. J. Heyd, E. N. Brothers, K. N. Kudin, V. N. Staroverov, T. A. Keith, R. Kobayashi, J. Normand, K. Raghavachari, A. P. Rendell, J. C. Burant, S. S. Iyengar, J. Tomasi, M. Cossi, J. M. Millam, M. Klene, C. Adamo, R. Cammi, J. W. Ochterski, R. L. Martin, K. Morokuma, O. Farkas, J. B. Foresman, D. J. Fox, *Gaussian 16*, Revision A.03, Gaussian, Inc., Wallingford CT, 2016.

[2] a) A. D. Becke, *J. Chem. Phys.* **1993**, *98*, 5648-5652; b) C. Lee, W. Yang, R. G. Parr, *Phys. Rev. B* **1988**, *37*, 785-789.

[3] P. C. Hariharan, J. A. Pople, *Theoret. Chim. Acta* **1973**, *28,* 213-222.

[4] H. Wu, Y. Wang, B. Song, H.-J. Wang, J. Zhou, Y. Sun, L. O. Jones, W. Liu, L. Zhang, X. Zhang, K. Cai, X.-Y. Chen, C. L. Stern, J. Wei, O. K. Farha, J. M. Anna, G. C. Schatz, Y. Liu, J. F. Stoddart, *Nat*. *Commun*. **2021**, *12*, 5191.

[5] X.-K. Ma, W. Zhang, Z. Liu, H. Zhang, B. Zhang, Y. Liu, *Adv*. *Mater*. **2021**, *33*, 2007476.

[6] X.-K. Ma, X. Zhou, J. Wu, F.-F. Shen, Y. Liu, *Adv*. *Sci*. **2022**, *9*, 2201182.

[7] H. Liu, M. Lin, Y. Cui, W. Gan, J. Sun, B. Li, Y. Zhao, *Chem*. *Commun*. **2021**, *57*, 10190-10193